

1 **Camphor Pathway Redux: Functional Recombinant Expression of 2,5- and 3,6-Diketocamphane**
2 **Monooxygenases of *Pseudomonas putida* ATCC 17453 with Their Cognate Flavin Reductase**
3 **Catalyzing Baeyer-Villiger Reactions**

4

5 Hiroaki Iwaki,¹ Stephan Grosse,² H el ene Bergeron,² Hannes Leisch,² Krista Morley,²

6 Yoshie Hasegawa,¹ and Peter C.K. Lau^{*2,3,4}

7

8 *Department of Life Science & Biotechnology and ORDIST, Kansai University, Suita, Osaka, 564-8680,*

9 *Japan,¹National Research Council Canada, Montreal, Quebec H4P 2R2, Canada,² McGill University,*

10 *Departments of Chemistry and Microbiology & Immunology, McGill University, Montreal, Quebec H3A*

11 *2B4, Canada³, and FQRNT Centre in Green Chemistry and Catalysis, Montreal, Quebec, Canada⁴*

12

13

14 Running title: CAMPHOR PATHWAY TYPE II BVMOs

15

16

17

18

19

20

21

22

23

24

25

26 **Abstract** Whereas the biochemical properties of the monooxygenase components that catalyze
27 the oxidation of 2,5-diketocamphane and 3,6-diketocamphane (2,5-DKCMO and 3,6-DKCMO,
28 respectively) in the initial catabolic steps of (+) and (-) isomeric forms of camphor metabolism
29 in *Pseudomonas putida* ATCC 17453 are relatively well characterized, the actual identity of the
30 flavin reductase (Fred) component that provides the reduced flavin to the oxygenases is hitherto
31 ill-defined. In this study, a 37-kDa Fred was purified from camphor-induced culture of *P. putida*
32 ATCC 17453 and this facilitated cloning and characterization of the requisite protein. The active
33 Fred is a homodimer with a subunit molecular mass of 18-kDa that uses NADH as electron
34 donor ($K_m = 32 \mu\text{M}$) and it catalyzes the reduction of FMN ($K_m = 3.6 \mu\text{M}$; $k_{\text{cat}} = 283 \text{ s}^{-1}$) in
35 preference to FAD ($K_m = 19 \mu\text{M}$; $k_{\text{cat}} = 128 \text{ s}^{-1}$). Sequence determination of ~40-kb of the
36 camphor (CAM) degradation plasmid revealed the locations of two isofunctional 2,5-DKCMO
37 genes (*camE*₂₅₋₁ for 2,5-DKCMO-1, and *camE*₂₅₋₂ for 2,5-DKCMO-2) as well as that of 3,6-
38 DKCMO-encoding gene (*camE*₃₆). In addition, by pulsed-field gel electrophoresis, the CAM
39 plasmid was established to be linear and ~533-kb in length. To enable functional assessment of
40 the two-component monooxygenase system in Baeyer-Villiger oxidations, recombinant plasmids
41 expressing Fred in tandem with the respective 2,5-DKCMO and 3,6-DKCMO encoding genes in
42 *Escherichia coli* were constructed. Comparative substrate profiling of the isofunctional 2,5-
43 DKCMOs did not yield obvious differences in Baeyer-Villiger biooxidations but they are distinct
44 from 3,6-DKCMO in the stereoselective oxygenations with various mono- and bicyclic ketone
45 substrates.

46

47 INTRODUCTION

48 In the history of *Pseudomonas* genetics, camphor metabolism by *P. putida* ATCC 17453
49 (NCIMB 10007; referred herein as strain PpCam), mediated by the “large” incompatibility group
50 2 (incP2) transmissible CAM plasmid, may be regarded as the genus’ oldest known profession
51 (1-3). Pioneering work by the laboratory of the late Gunsalus and coworkers dated back half a
52 century ago (1, 4-6) A schematic representation of the catabolic steps of conversion of the (+)
53 and (-) isomeric forms of camphor (compounds **1** and **2**, respectively) in strain PpCam that
54 includes contributions from this study is shown in Fig. 1. In this pathway, the genetics and
55 biochemistry of the cytochrome P450-containing enzyme complex (CamCAB) and 5-*exo*-
56 hydroxycamphor dehydrogenase (CamD) that led to the formation of the 2,5-diketocamphane or
57 3,6- diketocamphane (compounds **3** and **4**, respectively in Fig. 1) are well understood (7-12).

58 Metabolism of compound **3** or **4** proceeds via the action of a Baeyer-Villiger monooxygenase
59 (BVMO) system known as 2,5-diketocamphane monooxygenase (2,5DKCMO) or 3,6-
60 diketocamphane monooxygenase (3,6-DKCMO) (9, 13, 14). Both are prototype members of type
61 2 BVMOs (15) the fact that they are FMN and NADH-dependent, in sharp contrast to the more
62 frequently found type 1 BVMOs that use FAD as a prosthetic group and NADPH as a cofactor.
63 BVMOs in general are virtuous green reagents (using molecular oxygen as oxidant and
64 producing only water as a byproduct) that have a proven record of assessing high chemo-, regio-
65 and enantio-selectivity in a variety of oxidation reactions that include epoxidation and S- and N-
66 heteroatom oxidations (16-20).

67 It is generally known that either 2,5-DKCMO or 3,6-DKCMO consists of a homodimeric
68 FMN-containing oxygenation component and a second component that has been referred to as
69 an NADH dehydrogenase or NADH oxidase (14) which may be common to both flavoproteins.

70 In keeping with the modern nomenclature of the FMN-dependent two-component
71 monooxygenase systems (21), we adopt the name flavin reductase or Fred in this study.
72 Both the DKCMO oxygenating subunits of strain PpCam have been purified to homogeneity and
73 shown to be discrete enzymes having different molecular weights (subunit M_r 37-40 kDa vs. 38-
74 40.3 kDa) and isoelectric points (4.6 vs. 5.5) (9, 13, 14). Also, both DKCMOs have been
75 crystallized, but only the structure of 3,6-DKCMO has been solved to 2.00 Å resolution (PDB id:
76 2wgk, 22-24). Recently, Kadow et al (25, 26) described the gene structures of a 2,5-DCKMO
77 and 3,6-DCKMO and reported biotransformation results based on a presumed endogenous
78 reductase from the *Escherichia coli* host that could complement the DKCMO activity. Needless
79 to say, without a *bona fide* reductase the reported activities were extremely low if at all reliable.
80 Indeed, the majority of the biotransformation experiments carried out in the past by pioneering
81 lab of Willetts using the two enantiomeric systems had been conducted in whole *P. putida* cells.
82 A mixture of the 2,5-DKCMO and 3,6-DKCMO enzymes has been referred to as MO1 to
83 distinguish it from the MO2 activity of 2-oxo- Δ^3 -4,5,5-trimethylcyclopentylacetyl-CoA
84 monooxygenase (OTEMO), a type 1 BVMO (15, 26-29). Importantly, each DKCMO enzyme
85 was shown to have absolute specificity for substrates of the respective enantiomeric series of
86 camphor-ketones and also shown to have useful enantioselective properties (27, 30-33). These
87 enzymes are also active on the respective camphor enantiomer (13, 14, 34).

88 The following are brief accounts of previous attempts to isolate the reductase component of
89 the DKCMO system. Conrad et al (4-6) described this as an “electron transport oxidase”
90 believed to catalyze the FMN-mediated reduction of oxygen to hydrogen peroxide by NADH.
91 However, Trudgill et al. (35, 36) demonstrated that this enzyme of 36-kDa purified from (+)-
92 camphor grown cells of *P. putida* strain C₁B (= ATCC 17453; 13, 14, 22) did not directly

93 transfer electrons to oxygen and introduced the name NADH:(acceptor) oxidoreductase; also
94 known by its trivial name as NADH dehydrogenase. The purified enzyme was found to bind
95 FMN very weakly (K_d of 0.45 μ M) in a 1:1 ratio. It was further characterized to contain two
96 flavin-binding sites and would loosely interact with the oxygenating component to form an
97 active complex. Since these studies there had been no further work on the enzyme.

98 In this study we set out to identify and clone the gene for a flavin reductase (Fred) from strain
99 PpCam that is requisite to oxygenating activity. The new Fred-encoding gene was assembled
100 with the corresponding DKCMO gene for the first time to facilitate Baeyer-Villiger oxidations in
101 a recombinant format. In addition, we applied pulsed-field gel electrophoresis to uncover new
102 salient features of the prototypical CAM plasmid. This study was also set out to sequence CAM
103 plasmid DNA beyond the well established but limited *cam* operon locus with the goal to
104 localize the positions of the 2,5- and 3,6-DKCMO encoding genes with respect to both known
105 and potential new genes that may be assigned to the complete CAM degradation pathway.

106

107 MATERIALS AND METHODS

108 **Bacterial strains and culture conditions.** *P. putida* ATCC 17453 (strain PpCam) and *E. coli*
109 strains were grown at 30 °C and 37 °C, respectively, and routinely cultured in Luria-Bertani
110 (LB) broth or media as previously described (29). When necessary, the media were
111 supplemented with ampicillin (Ap, 100 μ g/ml). Growth of strain PpCam on (+) or (-) or racemic
112 camphor (0.3-0.5%) as sole carbon source was carried out in mineral medium as originally
113 described (13, 14).

114 **CAM plasmid size determination.** Megaplasmid detection was first performed using the in-
115 well cell lysis technique (37) as described in the supplemental material accompanying Fig. S2.

116 To determine the molecular sizes of the large plasmids, their profiles were determined by
117 using nuclease S1 treatment followed by pulsed-field gel electrophoresis (PFGE) as originally
118 described by Barton et al. (38) with some modifications. Briefly, genomic DNAs of
119 *Sphingomonas aromaticivorans* F199 used as control (39) and PpCam were first embedded in
120 agarose plugs. To linearize potential circular megaplasmids, 4 mm slices of agarose plugs were
121 cut out and equilibrated in S1 buffer (50 mM NaCl, 30 mM sodium acetate, pH 4.5, 5 mM
122 ZnSO₄) for 30 min, and then digested with 8 U of *Aspergillus oryzae* S1 nuclease (Fermentas
123 EN0321) for 15 min at 37 °C. Slices of the plug incubated only in S1 buffer were run in parallel
124 to detect non-linearized megaplasmids. The reaction was stopped by the addition of 20 µL of
125 EDTA (0.5 M, pH 8). The plugs were loaded immediately on a 0.8% agarose gel in 1x TBE
126 buffer and the wells were sealed by addition of agarose. The gel was run at 4 °C for 65 hours
127 using a Q-Life Autobase PFGE system with ROM card No. 5 for resolution of 100- to 1100-kb
128 DNA fragments (40). The gel was stained with 0.5 µg/mL ethidium bromide for 1 hour, washed
129 in distilled water for 50 min, then photographed.

130 **Cloning and sequencing of additional genes in the CAM pathway.** Recombinant
131 techniques were carried out according to Sambrook et al (41). Cloning and localization of the
132 2,5-DKCMO-1 encoding gene in a 6.8-kb BamHI fragment of PpCam total DNA in an *E. coli*
133 recombinant plasmid pCAM200 has been described previously (29). Additional cloning of a
134 ~26-kb DNA segment of PpCam DNA downstream of the *camDCAB* operon in four overlapping
135 clones (13-kb BamHI fragment in pCAM300; 5.5-kb Nsi fragment in pCAM500; 8.1-kb BamHI
136 fragment in pCAM600; and 7.1-kb BglII fragment in pCAM700), and analysis of the DNA
137 sequence determination are described in the supplemental material SM1/TableS1/Table S2. A
138 summary of the established and predicted gene organization is shown in Fig. 2.

139 **Construction of overexpression clones of DKCMOs.** The isopropyl- β -D-
140 thiogalactopyranoside (IPTG)-inducible *E. coli* pSD80 vector (42) was used to carry the
141 respective *Pfu* DNA polymerase-amplified DKCMO-encoding genes using the forward and
142 reverse primers with built-in EcoRI or PstI restriction sites listed in Supplemental material Table
143 S1. The resulting clones transformed in *E. coli* BL21 cells are designated pDKCMO25-1,
144 pDKCMO25-2, and pDKCMO36, respectively. The cloned inserts were verified by DNA
145 sequencing as previously described (43, 44).

146 **Purification of recombinantly produced DKCMOs.** All purification procedures were
147 performed at 4 °C on an ÄKTAexplorer™ 100 Air chromatography system (GE Healthcare).
148 Crude enzyme extract of the respective stock culture was processed essentially as previously
149 described for OTEMO (29). A three-step purification scheme that led to electrophoretic purity of
150 the proteins was developed as described in the supplemental material that accompanies Fig S4.

151 **CD spectroscopy and determination of melting point (T_m).** CD spectra of the DKCMOs
152 were recorded on a Jasco J-815 spectrometer operating with the Spectra Manager software.
153 Temperature was controlled by a Jasco PFD-452S peltier unit. Purified protein solutions were
154 desalted using a HiPrep Desalting column (26/10) previously equilibrated with 20 mM Na-
155 Phosphate buffer (pH 7.0). Final protein concentration was adjusted to about 0.1 mg/ml and the
156 respective CD spectrum was recorded between 200 and 260 nm using a Quartz cuvette (ID = 0.1
157 cm). Blanks containing buffer only were prepared and used as baseline. Temperature dependent
158 protein unfolding was monitored at 222 nm with thermal profiles ranging from 20 to 80 °C (2°C
159 min⁻¹). Thermodynamic parameters (T_m , ΔH , ΔS , ΔG) were calculated using the Spectra
160 Manager software.

161 **DKCMO cell free assays.** Enzyme activity was routinely detected in a reaction mixture (0.5
162 mL) containing Tris/HCl buffer (50 mM, pH 7.5), 3.3 mM NADH, 0.03 mM FMN, 30 mU of
163 formate dehydrogenase (FDH), 50 mM sodium formate, 10-50 mU Fred and about 0.4 mg of the
164 respective DKCMO. The reaction was started by adding (+)-camphor (2 mM) for the 2,5-
165 DKCMOs and (-)-camphor for 3,6-DKCMO, respectively. Controls contained all components,
166 but DKCMO or Fred. Samples were incubated for 10, 20, 30, 60, 90 min, respectively, and
167 reaction was stopped by adding 0.5 ml of acetonitrile. Precipitated protein was removed by
168 centrifugation and substrate depletion was followed by HPLC using a C₁₈ column. An isocratic
169 method was used with H₂O/CH₃CN/CH₃COOH (598/400/2) as mobile phase (0.5 ml/min) and
170 UV-detection at 220 nm on a Waters Millennium system.

171 **Detection and purification of an FMN-reductase (Fred) from strain PpCam.** Fred
172 activity was assayed in a reaction mixture (1 ml) containing Tris/HCl buffer (50 mM, pH 7.5),
173 0.07 mM NADH, and 0.025 mM FMN, and the reaction initiated by the addition of an
174 appropriate amount of enzyme. The decrease in absorbance at 340 nm due to the oxidation of
175 NADH was monitored. Blanks containing all components except the substrate (FMN) were
176 prepared. Specific activity was defined as the amount of protein that oxidizes one μ mole of
177 NADH ($\epsilon = 6.22 \text{ L mmol}^{-1} \text{ cm}^{-1}$) per minute (U) per milligram of protein (U/mg).

178 Purification of Fred was performed at 4 °C on an ÄKTAexplorer™ 100 Air chromatography
179 system (GE Healthcare). The crude extract of (+)-camphor grown culture of PpCam obtained by
180 cell breakage via French press was loaded on a DEAE-Sepharose FF column (XK50/20)
181 equilibrated with 20 mM sodium phosphate buffer (pH 7.0). The flow rate was 4 ml/min. The
182 column was washed with the same buffer until no protein could be detected in the flow through,
183 and enzyme was subsequently eluted with a linear gradient of 0 – 0.2 M NaCl. Active fractions

184 were pooled and concentrated by ultrafiltration (200 mL stirring cell, Amicon, USA, using a
185 YM3 membrane) and applied to a Ni-NTA column (16/10) previously equilibrated with 20 mM
186 sodium phosphate buffer containing 0.15 M NaCl. The flow through containing the active
187 protein was collected, concentrated and applied to a HiLoad Superdex 200 prep grade column
188 (16/60) which was previously equilibrated with 20 mM sodium phosphate buffer (pH 7.0)
189 containing 0.15 M NaCl. Protein was eluted with the same buffer (flow rate of 1.5 mL/min) and
190 collected in 2 ml fractions.

191 **Kinetic parameters.** Kinetic parameters of the Fred were determined by using the double-
192 reciprocal transformation (Lineweaver-Burk plot) of the Michaelis-Menten equation under
193 steady-state conditions. Results were verified by Eisenthal-Cornish-Bowden direct plots. Initial
194 reaction rates were measured at 25 °C in Tris/HCl buffer (50 mM, pH 7.5) by using total
195 substrate and coenzyme concentration between 1-100 μM, respectively.

196 **N-terminal and internal peptide sequencing and chemical digestion of Fred.** Purified
197 Fred, separated by SDS-PAGE was blotted to a polyvinylidene difluoride (PVDF) membrane
198 (Bio-Rad, USA). N-terminal sequence determination was performed with a sequencer (473A;
199 Applied Biosystems) by the Edman method (45). Phenylthiohydantoin amino acids were
200 analyzed by HPLC with a reversed-phase column. For internal peptide sequencing, purified Fred
201 was adjusted to 1 mg/ml and chemically digested using the following chemicals: o-iodobenzoic
202 acid (46), cyanogen bromide (47), and formic acid (48). Cleaved protein fragments were
203 separated by SDS-PAGE (15% PA), and peptide sequences of the cleaved protein fragments
204 were determined as described above.

205 **Cloning of the flavin reductase-encoding gene (*fred*) from strain PpCam.** Two primers
206 with the following sequences were designed based on the determined peptide sequences,

207 ATDPQWF and PPLVAF, respectively: fRED07-5'spec and 2SG-REV1 (Table S1). Following
208 the addition of a 3'-overhang, the amplified 150-bp product was cloned in the TOPO TA cloning
209 vector pCR2.1-TOPO (Invitrogen cat.:#K4500-01) and transformed in *E. coli* Top 10, and the
210 resulting plasmid was designated pCR2.1TOPO-frgPCR G1#3 and sequenced to confirm its
211 identity. To clone the complete *fred* gene, the GenomeWalker Universal Kit (Clontech #cat:
212 638904) was utilized and genomic libraries from strain PpCam were generated by digestion with
213 different blunt end cutting endonucleases (EcoRV, PvuII and StuI) and by adapter ligation at the
214 ends of the resulting DNA fragments. These libraries were utilized as independent templates in
215 three different PCR reactions. One gene specific primer, GSP1RED (Table S1) from the
216 pCR2.1TOPO-frgPCR G1#3 sequence was used in combination with a kit adapter primer (AP1)
217 in a first PCR reaction. Subsequently, 1 μ L of the first PCR (diluted 50-fold) served as a
218 template in a secondary PCR, applying one nested gene-specific primer, GSP2RED (Table S1)
219 along with a nested kit adapter primer (AP2). The resulting products were cloned into pCR2.1-
220 TOPO and the sequences of the inserts were determined.

221 The DNA fragment carrying *fred* was amplified by using Platinum *Pfx* DNA polymerase
222 (Invitrogen) with two PCR primers with NdeI and EcoRI restriction sites (fred07Nde-f and
223 fred07Eco-r in Table S1) to facilitate subsequent cloning. The amplified DNA fragment was
224 purified from agarose gel, digested with the restriction enzymes and cloned in the pET17b
225 vector. *E. coli* BL21(DE3)/pLysS containing the plasmid pET-Fred07#3 was cultivated in 250
226 mL of LB medium containing 100 μ g/mL of ampicillin at 30 °C. When the culture reached an
227 OD₆₀₀ of 0.6, IPTG was added to a final concentration of 1 mM in the medium. The cells were
228 further cultured overnight, then harvested by centrifugation.

229 **Construction of tandem clones: CamE₂₅₋₁+Fred, CamE₂₅₋₂+Fred and CamE₃₆+Fred in**
230 **pSD80.** All tandem clones were constructed using the MultiSite Gateway® Pro Kit (Invitrogen).
231 For each DKCMO (CamE) clone, the *tac* promoter and the specific *camE* gene were amplified
232 with Platinum Pfx DNA polymerase (Invitrogen) as follows: the forward primer attB1MO (Table
233 S1) and the reverse primers: attB5rMO1, attB5rMO2, and attB5rMO3 (Table S1) for *camE₂₅₋₁*,
234 *camE₂₅₋₂*, and *camE₃₆*, respectively. The templates used for the amplification are clones
235 pDCKMO25-1, pDKCMO25-2, and pDCKMO36. The T7 promoter and *fred* gene were
236 amplified with Platinum Pfx DNA polymerase (Invitrogen) and the primers: attB5fred, and
237 attB2fred (Table S1). The template for amplification was clone pET17b-Fred as described in the
238 previous section.

239 The various *camE* PCR products were recombined with the pDONR 221 P1-P5r Gateway
240 vector (Invitrogen) in separate reactions to form entry clones pDONR(2,5DKCMO-1),
241 pDONR(2,5DKCMO-2), and pDONR(3,6-DKCMO), respectively. The *fred* PCR product was
242 recombined with the pDONR 221 P5-P2 vector to form entry clone pDONR(Fred07).
243 pDONR(2,5-DKCMO-1) and pDONR(Fred07) were recombined with the pSD80 destination
244 vector, which was constructed using the Gateway Vector Conversion System (Invitrogen) via
245 ligation of the RfA cassette (provided in the kit) with vector pSD80, which had been linearized
246 with the restriction enzyme BamHI and blunt-ended with T4 DNA polymerase. The
247 recombination product of the three plasmids was transformed into One Shot® Mach1™ T1^R
248 chemically competent *E. coli*. The plasmid containing the double clone (pSD80-CamE₂₅₋₁-Fred)
249 was then transformed into *E. coli* BL21(DE3) for protein expression. Identical procedures were
250 carried out for the recombination of pDONR(2,5-DKCMO-2) and pDONR(3,6DKCMO) with

251 pDONR(Fred07) and the pSD80 destination vector to afford plasmids pSD80-CamE₂₅₋₂-Fred and
252 pSD80-CamE₃₆-Fred, respectively.

253 **Monooxygenase-catalyzed BV oxidations.** *E. coli* BL21 harboring the respective
254 monooxygenase (2,5-DKCMO-1, 2,5-DKCMO-2, and 3,6-DKCMO) and Fred containing
255 plasmid was maintained on LB medium containing glycerol (50%, vol/vol) at – 80 °C. For
256 biotransformation experiments, a fresh LB agar plate (1.5% agar) containing ampicillin (100
257 µg/ml) was prepared from the stock culture, and one colony was transferred to a preculture (20
258 ml) containing LB medium supplemented with ampicillin (100 µg/ml) and grown at 30 °C at 200
259 rpm on an orbital shaker overnight. An aliquot of the suspension (2 ml) was used to inoculate LB
260 medium (200 ml) supplemented with ampicillin (100 µg/ml) and the resulting suspension was
261 grown at 30 °C at 200 rpm on an orbital shaker. At an OD₆₀₀ of 0.5 (~ 3 h) protein expression
262 was induced by the addition of IPTG (final concentration 1 mM). The cells were allowed to grow
263 for an additional 3 hours (OD₆₀₀ of 2.0 - 2.2), and the cell suspension was divided into 10 ml
264 batches. To each batch a solution of substrate in isopropanol (1 M, 30 µl) was added and the
265 reaction flask was shaken at 30 °C at 200 rpm on an orbital shaker. After 18 hours the cell
266 suspension was centrifuged and the supernatant was extracted with ethyl acetate (10 ml). The
267 layers were separated and the organic layer was dried over anhydrous sodium sulphate and
268 filtered. The obtained solution was used for GC analysis. For retention times of starting materials
269 and products, and details on the GC analysis, readers are referred to Supplemental material SM2.

270 **Accession numbers.** The nucleotide sequences determined in this study have been deposited
271 in the Genbank database under accession numbers AB771747 and KC349947.

272

273 **RESULTS**

274 **Linear nature of CAM plasmid.** The CAM plasmid extracted by in-well cell lysis was first
275 analyzed by traditional agarose gel electrophoresis and seen to migrate as a discrete band as well
276 as those of the two circular plasmids of *S. aromaticivorans* strain F199 strain (pNL1 and pNL2)
277 that were used as control (Fig. S2 in supplemental material). Next, S1 nuclease was used to
278 linearize circular plasmids and analyzed on PFGE. As a result, two bands corresponding to the
279 linearized pNL1 and pNL2 plasmids, calibrated by linear markers as between 145.5-194-kb, and
280 485-kb, respectively, are visible for the F199 strain treated with S1 nuclease (Fig. 3, lane 3). No
281 such resolution was observed for the S1 nuclease untreated sample as expected of large circular
282 plasmids (lane 2). On the other hand, both the S1-treated (lane 5) and non-treated (lane 4)
283 samples of CAM plasmid afforded one band estimated at 533 kb, indicating that the CAM
284 plasmid is linear. Further, the migration of CAM plasmid exhibited constant mobility relative to
285 the particular size marker under other pulse conditions (not shown).

286 **Sequenced locus, gene context and characteristics of 2,5-DKCMOs and 3,6-DKCMO.** In
287 total, a 40,450-bp region of the pCAM plasmid is now available as a result of cloning and
288 sequencing various DNA fragments encompassing the established *camRDCAB* locus (Fig. 2).
289 Except for the 2,5-DKCMO and 3,6-DKCMO-encoding genes described below, characteristics
290 of the other predicted open reading frames (ORFs) which may account for additional
291 biochemical steps of the CAM pathway are given in Table S2 and Fig. S1 of the supplemental
292 material.

293 As previously reported, a 2,5-DKCMO-encoding gene (now referred to as *camE₂₅₋₁* for 2,5-
294 DKCMO-1) was localized 88-bp downstream of the OTEMO-encoding gene (*camG*) and likely
295 co-transcribed (29). Herein we report the presence of a second copy of 2,5-DKCMO (*camE₂₅₋₂*;

296 for 2,5-DKCMO-2) that is localized some 23-kb downstream and encoded on an opposite strand,
297 implying divergent transcription (Fig. 2). In the same DNA strand, and separated by two
298 potential ORFs downstream, the 3,6-DKCMO encoding gene (*camE₃₆*) was identified. The 378-
299 amino acid protein sequence of 3,6-DKCMO was previously deposited in the RCSB protein data
300 bank as code 2WGK (www.pdb.org) that described the dimeric structure of the protein (24).
301 Identification of the N-terminal portion of this protein was aided by the available 29-amino acid
302 peptide sequence (15, 31) with one mismatch (arginine to alanine change at position 20
303 numbered from the first methionine). It is noteworthy that the subunit structure of 3,6-DCKMO
304 was superimposable with the α -subunit of luciferase with an root-mean-square deviation
305 (RMSD) of 1.83 Å (253 matching C ^{α} atoms out of 378) (24).

306 The nucleotide sequences of *camE₂₅₋₁* and *camE₂₅₋₂* are 90% identical, the base changes result
307 in 28 amino acid substitutions along the 363-amino acid polypeptide, of which 18 are
308 conservative changes (Fig. S3a in supplemental material). Interestingly, the predicted N-terminal
309 20 amino acid sequence of 2,5-DKCMO-2 instead of 2,5-DKCMO-1 matches more closely to
310 the peptide sequence obtained by N-terminal sequencing of what was then known as 2,5-
311 DKCMO, a single protein (15, 31). The QA dipeptide at positions 2 and 3 are key determinants
312 (Fig S3b in supplemental material).

313 Approximately half of the 2,5-DKCMO and 3,6-DCKMO polypeptide sequences are
314 conserved (43.3-44.4% identity and 59.6-60.6% overall similarity), notably the presence of two
315 conserved stretches of 10 and 14 amino acids and a major deletion of 12 amino acids near the N-
316 termini of both 2,5-DKCMOs (Fig. S3a in supplemental material). A comparison of the predicted
317 secondary structures between the 2,5-DKCMO isozymes and 3,6-DKCMO shows that sequence

318 divergence appears to be localized in the extreme N-terminal region and around the
319 deletion/insertion region.

320 During the process of isolation from the respective overproducing clones, all three proteins
321 exhibited the characteristic intense yellow color of flavoproteins; however, the prosthetic group
322 (FMN) appeared to be loosely bound to the proteins. When loaded on a hydrophobic column
323 (Butyl-S-Sepharose) to which the proteins bind, FMN was eluted as a clear yellow band upon
324 washing. The now colorless enzymes, however, remained fully active in the *in vitro* assay where
325 exogenous FMN was added. Some 25 mg/L of purified 2,5-DKCMO-2, 50 mg/L of each of 2,5-
326 DKCMO-1 and 3,6-DKCMO could be obtained from the respective overproducing clones. On
327 SDS-PAGE, the purified 2,5-DKCMOs showed a M_r of 41- kDa for either isozyme (theoretical
328 40,702 and 40,574, respectively) and 44-kDa for the 3,6-DKCMO (theoretical, 42,311) (Fig. S4
329 in supplemental material). That 2,5-DKCMO is not larger than 3,6-DKCMO agrees with the M_r
330 estimated from the respective His-tagged proteins (25). Native M_r analyzed on HiLoad Superdex
331 200pg were estimated as 60-kDa, 64-kDa and 85-kDa, respectively (Fig. S5 in supplemental
332 material) supporting the dimeric nature of the proteins as previously reported (13, 14, 22, 23).

333 All 3 DKCMOs exhibit the typical CD spectrum of proteins with α -helices as the predominant
334 form of secondary structure (Fig. S6a in supplemental material). They all show minima at 222nm
335 and 208nm with a near identical profile for the two 2,5-DKCMOs but somewhat different for the
336 3,6-DKCMO especially at 208nm wavelength. Monitoring the CD at a fixed wavelength of
337 222nm while varying temperature allowed for the visualization of the protein unfolding process.
338 Interestingly, the resulting estimated melting temperatures (T_m) of the proteins (the temperature
339 where folded and unfolded protein are in equilibrium) differed substantially. These are 56 ± 1 °C,
340 63 ± 1 °C, and 47 ± 1 °C, for 2,5-DKCMO-1, 2,5-DKCMO-2 and 3,6-DKCMO, respectively (Fig

341 S6b). By virtue of a 7°C higher T_m than that of 2,5-DKCMO-1 in the thermal denaturation
342 experiments it can be anticipated that 2,5-DKCMO-2 has a longer shelf life time than the other
343 counterpart.

344 **Identification, purification and properties of Fred.** In crude extracts of strain PpCam
345 grown on (+)-camphor, FMN reductase activity (see Materials and methods for details) was
346 detected which seemed to originate from only one enzyme that we designated Fred. This activity
347 was not detected when the strain was grown with glucose as sole carbon source. This enzyme
348 was subsequently purified to homogeneity using a 3-step procedure with a yield of 18% (Fig. 4).
349 The specific activity (628.4 U/mg) of the purified Fred represents a ~260-fold purification. In the
350 purification process a major contaminating protein was experienced during the DEAE-Sepharose
351 chromatography where medium components and about 90% of unspecific proteins were
352 removed. This protein that co-eluted with Fred was subsequently identified by N-terminal
353 sequencing as camphor-5 monooxygenase (P450_{cam}) which is known to be induced upon growth
354 of strain PpCam on (+)-camphor. However, in the following Ni-NTA resin chromatography, this
355 major contaminant remained bound to the resin whereas the reductase flowed through which was
356 collected and concentrated. The resulting homogenous protein fraction containing Fred was a
357 clear solution showing a single absorbance maximum at 280 nm indicating it a non-flavoprotein.

358 The active Fred is a homodimeric protein with an apparent M_r of 37.2 kDa by size exclusion
359 chromatography on Superdex 200 (Fig. S7 of supplemental material) and a subunit M_r of ~18
360 kDa by SDS-PAGE (15% PA) analysis (Fig. 4). The pH optimum was 7.5 determined in
361 Tris/HCl buffer (50 mM). However, both activity and pH optimum appeared to depend on the
362 buffer used, e.g., at pH 7.5 in phosphate buffer the enzyme activity was reduced to 40%; in
363 piperazine-HCl (pH 5-6.5) and phosphate buffer (pH 6.5-7.5) both at 50 mM, Fred was found to

364 have an optimum activity at a lower pH of 5-6 (not shown). Optimum temperature for Fred
365 activity was seen at between 30 and 35 °C.

366 **Activation energy and thermostability.** An activation energy of 7 kcal mol⁻¹ was estimated
367 for the Fred reaction (Fig. S8 in supplemental material). Based on this data, a 10 °C increase of
368 the reaction temperature (ΔT_{10}) would result in about 1.5 times higher rate constant. At 25 °C the
369 free energy of activation (ΔG^\ddagger) was calculated to be 11.7 kcal mol⁻¹.

370 Fred was rather stable when stored at 4 °C over several days. However, at room temperature
371 (25 °C) the enzyme irreversibly unfolds with a half life of about 80 min (Fig. S9ab in
372 supplemental material). At higher temperature (between 30 and 35 °C) the half life of the
373 enzyme is even shorter, ~5-20 min.

374 **Substrate specificity and kinetic properties of Fred.** FMN and FAD are both substrates for
375 the reductase. However, the enzyme favors FMN demonstrated by a 2-fold higher rate constant
376 and about 5 times higher affinity ($K_m = 3.6 \mu\text{M}$, $k_{\text{cat}} = 283 \text{ s}^{-1}$, $k_{\text{cat}}/K_m = 7.9 \times 10^7$) when compared
377 to FAD ($K_m = 19 \mu\text{M}$, $k_{\text{cat}} = 128 \text{ s}^{-1}$, $k_{\text{cat}}/K_m = 6.7 \times 10^6$). With regard to electron donor, only
378 NADH is effective where NADPH in similar concentration acts as a very poor co-substrate. The
379 K_m for NADH was estimated to be 32 μM . NAD^+ is a competitive enzyme inhibitor with a
380 determined K_i of 40 mM.

381 **Cloning of Fred-encoding gene, its sequence characteristics and gene context.** Chemical
382 cleavage of purified Fred using cyanogen bromide or formic acid yielded six peptide fragments
383 (not shown), five of which were used to determine internal peptide sequences as well as N-
384 terminal sequencing of the intact protein. The iodobenzoic acid treated sample did not produce
385 any usable fragment. Degenerate primers were designed from the sequenced peptides to first
386 clone a part of the reductase gene and eventually the entire gene as described in Materials and

387 methods. In a sequenced 4.9-kb region, Fred is flanked by a potential GTP cyclohydrolase and
388 luciferase upstream, and three potential genes downstream, all being encoded on the same DNA
389 strand (Fig. S10 in Supplemental information). Fred was cloned using the pET17b vector
390 designated pET-Fred07#3 and overexpressed in *E. coli* BL 21(DE3)/pLysS.

391 Fred consists of 170 amino acids with a predicted M_r of 18,466 Da in good agreement with
392 the experimentally determined result (Fig. 4). Three peptide sequences corresponding to amino
393 acid positions 2-21, 8-29 and 45-68 helped to establish the identity of the protein (Fig. 5). A
394 characteristic flavin reductase motif GDH (49) is found at positions 136-138. A conserved YGG
395 motif (50) is found 5-7 residues away from the C-terminus. In the BLAST search, the closest
396 homolog (59% identity) is that of a “flavin reductase-like FMN binding protein” present in the
397 genome sequence of *N. aromaticivorans* DSM 12444 (Genbank: ABD25905.1). The closest
398 homolog whose structure has been determined is nitrilotriacetate monooxygenase component B
399 (189 amino acids; NTA-MoB) derived from *Mycobacterium thermoresistibile* that was
400 characterized as a homodimer with a split-barrel motif typical of short-chain flavin reductases
401 (PDB ID 3NFW; 51).

402 It is interesting that in a phylogenetic analysis, the PpCam Fred does not cluster with
403 predicted flavin reductase counterparts originating from various *Pseudomonas* spp., e.g., *P.*
404 *putida* F1 or strain KT2440, but rather cluster with those members of the α -proteobacteria
405 particularly the *Novosphingobium* and *Sphingomonas* genera (Fig. S11 in supplemental
406 information).

407 The PpCam Fred-encoding gene is not part of the 40-kb sequenced *cam* locus or elsewhere
408 by PCR-amplification of the isolated CAM plasmid DNA (not shown). The same 4-kb gene locus
409 is not found in any of the presently sequenced *P. putida* genomes so far (not shown).

410 **Co-expression of DKCMO and Fred and enzyme activities.** Evidence for protein co-
411 production of DKCMO tandemly expressed with Fred is shown in Fig. S12 of supplemental
412 material. Of the three enzyme pairs, 2,5-DKCMO-1 and Fred gave the clearest expression as
413 seen on the SDS-PAGE. For unknown reason, the expression level of 3,6-DKCMO appeared to
414 be the weakest. Nonetheless, the biotransformation experiments (described in a later section)
415 using whole cells support the co-expression of the two proteins. In contrast, whole cells
416 expressing these oxygenating components alone showed very little activity with (+)- or (-)-
417 camphor as substrate.

418 In cell-free assays that involved an NADH-regenerating system using formate dehydrogenase
419 (FDH) and sodium formate, addition of different amounts of Fred was seen to potentiate the
420 monooxygenase activity. As an example, a ~20-fold increase in 2,5-DKCMO-2 activity due to
421 the addition of Fred is shown in Fig. 6. In two other experiments, linear dependency on the
422 concentration of Fred in the oxidation of (+)- or (-)-camphor was shown (Fig. S13 in
423 supplemental material). These experiments also showed the high specificity of the respective
424 DKCMOs toward the camphor enantiomers. Moreover, a ratio of 4:1 (DKCMO:Fred) was found
425 to be optimal for measuring enzyme activity. The pH optimum for 2,5-DKCMO-1, 2,5-
426 DKCMO-2, and 3,6-DKCMO was estimated to be 7.5, 8.0 (Tris-HCl-buffer) and 7.0 (sodium
427 phosphate buffer), respectively (not shown). Under these conditions the activities of the purified
428 2,5-DKCMO-1 and 2,5-DKCMO-2 *in vitro* were determined to be nearly identical at 1.0 U/mg
429 and 1.1 U/mg for (+)-camphor. For 3,6-DKCMO this was 0.81 U/mg with (-)-camphor.

430 **Coupled DKCMO-Fred oxidations of selected ketones.** To establish the substrate
431 acceptance and enantioselectivity of the three DKCMOs, whole-cell oxidations were carried out
432 for 18 hours in shake flasks using 3 mM of various ketones. Reaction conversions and

433 enantiopurities of starting materials and products were determined by chiral-phase GC as
434 described in Materials and Methods.

435 **(i) Terpenones.** For (+)-camphor (**1**), 2,5-DKCMO-1-Fred and 2,5-DKCMO-2-Fred showed
436 full conversion under the reaction conditions and did not convert (-)-camphor (**2**) (Table 1).
437 Conversely, 3,6-DKCMO-Fred fully converted (-)-camphor to lactone (**2a**) and showed no
438 conversion of (+)-camphor (**1**). Similarly, 2,5-DKCMO and 3,6-DKCMO purified from
439 camphor-grown PpCam (13) were reported to be specific for (+)- and (-)-camphor, respectively.
440 All three double clones were unable to convert (+)-fenchone (**6**), (-)-fenchone (**7**), and (+)-
441 nopinone (**8**).

442 **(ii) 2-Substituted monocyclic ketones.** For the kinetic resolution of 2-substituted
443 cyclohexanones (**9** – **12**), 2,5-DKCMO-1-Fred afforded the highest conversions and
444 enantioselectivities among the three double clones (Table 2). 2,5-DKCMO-1-Fred oxidized the
445 (*R*)-enantiomer of 2-phenylcyclohexanone (**12**) with an $E > 200$. 2,5-DKCMO-2-Fred was also
446 highly selective for the (*R*)-enantiomer ($E > 200$), although the reaction proceeded to only 4%
447 conversion compared to 23% for 2,5-DKCMO-1-Fred. On the contrary, 3,6-DKCMO-Fred
448 oxidized both enantiomers of 2-phenylcyclohexanone (**12**) at the same rate ($E = 1$) and to only
449 2% conversion.

450 For the oxidation of alkyl-substituted cyclohexanones (**9** – **11**), all three clones were (*S*)-
451 selective, although 3,6-DKCMO-Fred only recognized 2-methylcyclohexanone (**9**) ($E = 3.2$) as a
452 substrate. 2,5-DKCMO-1-Fred and 2,5-DKCMO-2-Fred resolved 2-ethylcyclohexanone (**10**)
453 with good enantioselectivity ($E = 43$ and 22, respectively) and oxidized 2-propylcyclohexanone
454 (**11**) with moderate enantioselectivity ($E = 19$ and 8.5, respectively).

455 For the kinetic resolution of 2-alkylcyclopentanones (**13**, **14**), 2,5-DKCMO-1-Fred resolved
456 2-*n*-hexylcyclopentanone (**14**) with moderate enantioselectivity ($E = 19$) in favor of the (*S*)-
457 enantiomer. 2,5-DKCMO-2-Fred oxidized 2-*n*-hexylcyclopentanone (**14**) with low
458 enantioselectivity ($E = 5$), whereas no conversion was observed with 3,6-DKCMO-Fred. All
459 three clones were unable to convert 2-methylcyclopentanone (**13**).

460 **(iii) 4-Substituted cyclohexanones.** Biotransformations of 4-substituted cyclohexanones (**15**
461 - **18**) by 2,5-DKCMO-1-Fred, provided lactones with low to moderate ee values (Table 3).
462 Oxidation of 4-methylcyclohexanone (**15**) and 4-*n*-pentylcyclohexanone (**17**) resulted in 27%
463 and 26% ee of the respective (*R*)-lactones. Desymmetrization of 4-ethylcyclohexanone (**16**)
464 afforded the (*R*)-enantiomer in 71% ee, whereas the opposite enantiomer was obtained in 61% ee
465 for the oxidation of *tert*-butylcyclohexanone (**18**). 2,5-DKCMO-2-Fred also afforded the (*R*)-
466 lactone of 4-ethylcyclohexanone (**16**), although in significantly higher ee (89%). In contrast, the
467 (*S*)-lactone was obtained in 87% ee with 3,6-DKCMO-Fred. 2,5-DKCMO-2-Fred also oxidized
468 4-methylcyclohexanone (**15**) to the (*R*)-lactone (55% ee) but showed only traces of activity with
469 the remaining ketones. Similarly, 4-methyl, *n*-pentyl, and *tert*-butylcyclohexanone were not
470 substrates for 3,6-DKCMO-Fred.

471 **(iv) Bicyclic ketones.** The bioconversion of [3.2.0]hept-2-en-6-one (**19**) with 2,5-DKCMO-
472 1-Fred yielded the “normal” as well as the “abnormal” lactone in 1.3:1 ratio at 100% conversion
473 (Table 4). The “abnormal” lactone was obtained in excellent ee (99%), whereas the ee of the
474 “normal” lactone was significantly lower (77%). For 2,5-DKCMO-2-Fred, the “abnormal”
475 lactone was obtained in excellent ee (97%), and the ee of the “normal” lactone was also very
476 high (87%). Purified 2,5-DKCMO from the native strain, which we assume is composed of both
477 2,5-DKCMO-1 and 2, was reported to give the “normal” and “abnormal” lactones in a 1.3:1

478 ratio, with product ee values of 82% and 100%, respectively (28). 3,6-DKCMO-Fred gave a
479 1:1.5 ratio of “normal” and “abnormal” lactones at 53% conversion. The “abnormal” lactone was
480 obtained in 93% ee and the “normal” lactone was obtained in 57% ee. Purified 3,6-DKCMO
481 from the native strain (28) was reported to give a 1.3:1 ratio of “normal” and “abnormal”
482 lactones at 30% reaction conversion. The ee values of the “normal” (10% ee) and “abnormal”
483 (72% ee) lactones were significantly lower than obtained for the biotransformation with 3,6-
484 DKCMO-Fred.

485 For the oxidation of norcamphor (**20**) by 2,5-DKCMO-1-Fred, the “normal” lactone was
486 formed in a 2.4:1 ratio with the “abnormal” lactone at ~60% reaction conversion. Product ee
487 values were 40% ee and 57% ee, respectively. Biotransformation with 2,5-DKCMO-2-Fred
488 yielded the “normal” lactone in 58% ee and the “abnormal” lactone in 20% ee at 59% reaction
489 conversion. Purified 2,5-DKCMO was reported to give the “normal” lactone in 60% ee at 20%
490 reaction conversion (28). Formation of the “abnormal” lactone was not reported. 3,6-DKCMO-
491 Fred oxidized norcamphor exclusively to the “normal” lactone with excellent enantioselectivity
492 (94% ee) at 26% reaction conversion. Similarly, purified 3,6-DKCMO was reported to give the
493 “normal” lactone in >90% ee at 48 % conversion (28).

494

495 **DISCUSSION**

496 We have purified a camphor-inducible flavin reductase (Fred) from strain PpCam and this
497 homodimeric protein of subunit M_r of 18-kDa was shown to be functionally competent in
498 providing the required electrons to the respective monooxygenase component in the oxidation of
499 a variety of substrates. A chromosomally-located Fred-encoding gene was cloned and enabled
500 the first assembly of a *bona-fide* two-component system in a recombinant format for the

501 enantiomer-specific 2,5- and 3,6-DKCMOs. This DKCMO-Fred system represents the first
502 among the known FMN-dependent two-component monooxygenase systems (21) where a single
503 FMN reductase serves three separate monooxygenating components besides representing a single
504 step in the CAM degradation pathway (Fig. 1).

505 Contrary to a previously described oxidoreductase (14, 35, 36), Fred is not a flavoprotein.
506 The enzyme uses flavins (FMN in preference to FAD) only as substrates and thus it is not an
507 NADH oxidase and it is incapable of transferring electrons directly from NADH to molecular
508 oxygen. Fred also differs from the purified NADH oxidase (14, 35, 36) in that it is not a single
509 polypeptide of M_r 36-kDa but consists of two identical subunits of 18-kDa making it highly
510 unlikely that the homodimeric subunits would discriminate between FMN and FAD in regard to
511 their binding capacities: 1 mol/mol FMN, 2mol/mol FAD as described by Trudgill et al (35).
512 Other differences are in the isoelectric points (pI of 6.6 based on cellulose acetate electrophoresis
513 for NADH oxidase vs a theoretical pI of 4.97 for Fred), and the amino acid compositions (one
514 methionine, 4 half-cystines per mole of the former enzyme vs. the sequence-derived 4 cysteines
515 per subunit: 8 in total, and 4 methionines per subunit: 8 in total for Fred).

516 Characteristics of the strain PpCam Fred classify it a new member of the Class II
517 nonflavoprotein reductases, meaning that the flavin acts as a substrate for catalysis as opposed to
518 a tightly bound cofactor in Class I flavoprotein reductases (21, 52). The kinetic properties of
519 Fred toward FMN and NADH approximate those of FRD_H of *Beneckea harveyi* (52, 53). The
520 latter and a few others have been characterized to undergo a sequential mechanism of electron
521 transfer, i.e., the reduced flavin substrate is transferred to the monooxygenase component only
522 after its reduction by NADH (21). The conserved GDH motif in Fred implies that H136 may
523 play a critical role in NADH binding and reduction of the FMN cofactor, as it was first reported

524 for the NADH:flavin oxidoreductase (FRD_{Aa}) system of *Aminobacter animonvorans* (formerly,
525 NmoB or NtaB of *Chelatobacter heintzii*; 49). PpCam Fred also contains the conserved YGG
526 motif reported in the modeled structure of a flavin reductase of *Thermus thermophilus* HB8 that
527 uses FAD as substrate (50). This region was deemed important in substrate flavin binding by
528 deletion of the C-terminal 5 amino acids containing the YGG motif (50).

529 A second revelation of this study is the identification and localization of a duplicated set of
530 genes, *camE*₂₅₋₁ and *camE*₂₅₋₂ genes on the CAM plasmid that encode 2,5-DCKMO-1 and 2,5-
531 DKCMO-2. This unravels a 26-43 year old mystery first documented by Gunsalus and coworker
532 (54) and later by Trudgill (14) who although could not reproduce the presence of a “third”
533 component, referred to as E₂' in (54), provided electrophoretic evidence of two separable forms
534 of 2,5-DKCMO. The predicted charge difference between the two isozymes (pI 5.58 for
535 DCKMO-1 and 5.40 for DKCMO-2) would account for the electrophoretic separation in a native
536 gel (14). Clearly, the high sequence identity between *camE*₂₅₋₁ and *camE*₂₅₋₂ was the result of a
537 gene duplication event and sequence divergence in the case of *camE*_{3,6}. Identification of the
538 duplicated set of 2,5-DCKMO-encoding genes means that Kadow et al (25) had cloned the
539 *camE*₂₅₋₁ and all previously reported biotransformation results using whole cells of PpCam were
540 most likely the summation of the two DKCMO activities. Interestingly, the N-terminal amino
541 acid sequence experimentally determined for one DKCMO (15, 31) actually has a better match
542 to that of DKCMO-2 than DKCMO-1 (Supplemental material Fig. S3b).

543 With the reconstituted and “personalized” DKCMO-Fred plasmid systems we confirmed the
544 enantiomeric specificity of the 2,5-DCKMO and 3,6-DKCMO enzymes for the (+) and (–)
545 camphor as previously reported (13, 14). On the other hand, contradictory results were presented
546 by Kadow et al (25, 26) who relied on an unknown factor in *E. coli* to effect substrate oxidations.

547 Given the current spectrum of substrates, the oxidation effected by the two 2,5-DKCMO
548 isozymes so far appear indistinguishable. For synthetic purpose, most notable result is the
549 specificity toward the (*R*)-enantiomer of 2-phenylcyclohexanone (**12**) that rendered an *E* value of
550 >200 in both cases (Table 3). The action of 3,6-DKCMO is most different with regard to
551 oxidation of norcamphor (**18**) where it provided the “normal” lactone exclusively with excellent
552 enantioselectivity (94% ee) at 26% reaction conversion (Table 5).

553 Although CAM plasmid is widely known as one of the oldest known degradative plasmids
554 alongside SAL, NAH and OCT plasmids that are responsible for the degradation of salicylate,
555 naphthalene and octane, respectively (2, 55) its molecular size has been largely propagated in the
556 literature as 150-MDa or 236-250 kb (e.g. 25). Here, by the criteria of PFGE the CAM plasmid
557 was determined to have a size of ~530-kb, besides being linear. A covalently closed circular
558 plasmid would exhibit a constant migration pattern in the PFGE that is independent of the pulse
559 conditions (see SM2 note in supplemental material).

560 As per gene elucidation of the CAM degradation pathway, eight catabolic genes responsible
561 for four biochemical steps besides the regulatory *camR*, are now presently known and
562 characterized (8, 10-12, 24, 25, 29, this study). By sequence homology, additional ORFs that
563 could account for the remaining steps of the degradation pathway are presented in Fig. S3 of
564 supplemental material. It is interesting to note that besides the well characterized TetR-type
565 *camR* repressor that regulates the P-450cam hydroxylase operon (56), four potential
566 transcriptional repressors (orf5[CamS], orf11[CamU] and orf20[CamV] of TetR-type; and
567 orf7[CamT] of LysR-type) with limited sequence identity to each other with the exception of
568 Orf20[CamV] and CamR (54% identity), decorate the sequenced *cam* locus (Fig. 2). Clearly,
569 regulation of the entire *cam* pathway is complicated which is beyond the scope of this study.

570 Suffice it to say that the *camE*₂₅₋₁ and *camG* and those of *camE*₂₅₋₂ and *camE*₃₆ are predicted to be
571 divergently transcribed as per position on opposite DNA strand. Interestingly, this supports an
572 earlier observation that the MO1 (mixtures of 2,5- and 3,6-DKCMO) and MO2 (OTEMO)
573 activities are not “coordinately controlled.” (27).

574 In conclusion, the availability of the recombinant format of the three DKCMO-Fred systems
575 opens up new opportunities in organic synthesis besides the production of camphor lactones.
576 Access to exquisite sulfoxide synthons by “separated” DKCMO is a potentially grand
577 opportunity, made possible previously by using “washed whole cells” of strain PpCam (30).
578 With regard to mechanistic study, the new DKCMO-Fred systems provide an unique model for
579 structure-function analyses of a special enantiocomplementary kind where a single flavin
580 reductase serves three separate monooxygenating components. Are there differences in the
581 mechanism of flavin transfer from the reductase to the DKCMO enantiomeric pair is just one
582 more question in the complexity of flavoenzymology (21, 57).

583

584 **ACKNOWLEDGMENTS**

585 Funding by NRC through the National Bioproducts Program is gratefully acknowledged. This
586 work was financially supported in part by the Kansai University Expenditure for cultivating
587 young researchers (2012) provided to H. Iwaki. This paper is dedicated to the memory of late
588 Irwin C. (Gunny) Gunsalus (1912-2008), whose middle initial although stands for Clyde, should
589 be synonymous with camphor or cytochrome P450_{cam}.

590

591 **REFERENCES**

- 592 1. **Bradshaw WH, Conrad HE, Corey EJ, Gunsalus IC, Lednicer D.** 1959.
593 Microbiological degradation of (+)-camphor. *J. Am. Chem. Soc.* **81**:5507.
- 594 2. **Rheinwald JG, Chakrabarty AM, Gunsalus IC.** 1973. A transmissible plasmid
595 controlling camphor oxidation in *Pseudomonas putida*. *Proc. Natl. Acad. Sci. USA.*
596 **70**:885-889.
- 597 3. **Sokatch JR.** (1986) *The Bacteria*. Vol. 10. *The biology of Pseudomonas*. Acad. Press,
598 Inc. Harcourt Brace, Jovanovich, Publishers.
- 599 4. **Conrad HE, Dubus R, Gunsalus IC.** 1961. An enzyme system for cyclic ketone
600 lactonization. *Biochem. Biophys. Res. Commun.* **6**:293-297.
- 601 5. **Conrad HE, Dubus R, Namtvedt MJ, Gunsalus IC.** 1965. Mixed function oxidation.
602 II. Separation and properties of the enzyme catalysing camphor lactonization. *J. Biol.*
603 *Chem.* **240**:495-503.
- 604 6. **Conrad HE, Leib K, Gunsalus IC.** 1965. Mixed function oxidation. III. An electron
605 transport complex in camphor ketolactonization. *J. Biol. Chem.* **240**:4029-4037.
- 606 7. **Ougham HJ, Taylor DG, Trudgill PW.** 1983. Camphor revisited: Involvement of a
607 unique monooxygenase in metabolism of 2-oxo- Δ^3 -4,5,5-trimethylcyclopentenylacetic
608 acid by *Pseudomonas putida*. *J. Bacteriol.* **153**:140-152.
- 609 8. **Unger P, Sligar SG, Gunsalus IC.** 1986. *Pseudomonas* cytochromes P-450, p. 557-589.
610 *In* J.R. Sokatch (ed.), *The Bacteria*, Vol 10, Academic Press, New York.
- 611 9. **Trudgill PW.** 1986. Terpenoid metabolism by *Pseudomonas*. p483-525. *In* J.R. Sokatch
612 and L.N. Ornston (ed.), *The bacteria: a treatise on structure and function. The biology of*
613 *Pseudomonas*. Acad. Press. Inc. Orlando, Fla.

- 614 10. **Koga H, Aramakim H, Yamaguchi E, Takeuchi K, Horiuchi T, Gunsalus IC.** 1986.
615 *camR*, a negative regulator locus of the cytochrome P-450_{cam} hydroxylase operon. J.
616 Bacteriol. **166**:1089-1095.
- 617 11. **Koga H, Yamaguchi E, Matsunaga K, Aramaki H, Horiuchi T.** 1989. Cloning and
618 nucleotide sequence of NADH-putidaredoxin reductase gene (*camA*) and putidaredoxin
619 gene (*camB*) involved in cytochrome P-450_{cam} hydroxylase of *Pseudomonas putida*. J.
620 Biochem. **106**:831-836.
- 621 12. **Fujita M, Aramaki H, Horiuchi T, Amemura A.** 1993. Transcription of the *cam*
622 operon and *camR* genes in *Pseudomonas putida* PpG1. J. Bacteriol. **175**:6953-6958.
- 623 13. **Jones KH, Smith RT, Trudgill PW.** 1993. Diketocamphane enantiomer-specific
624 “Baeyer–Villiger” monooxygenases from camphor-grown *Pseudomonas putida* ATCC
625 17453. Gen. Microbiol. **139**:797-805.
- 626 14. **Taylor DG, Trudgill PW.** 1986. Camphor revisited: Studies of 2,5-diketocampane 1,2-
627 monooxygenase from *Pseudomonas putida* ATCC 17453. J. Bacteriol. **165**:489-497.
- 628 15. **Willetts A.** 1997. Structural studies and synthetic applications of Baeyer-Villiger
629 monooxygenases. Trends Biotech. **15**:55-62.
- 630 16. **Alphand V, Wohlgemuth R.** 2010. Applications of Baeyer-Villiger monooxygenases in
631 organic synthesis. Curr. Org. Chem. **14**:1928-1965.
- 632 17. **De Gonzolo G, Mihovilovic MD, Fraaije MW.** 2010. Recent developments in the
633 application of Baeyer-Villiger monooxygenases as biocatalysts. ChemBioChem **11**:2208-
634 2231.
- 635 18. **Leisch H, Morley K, Lau PCK.** 2011. Baeyer-Villiger monooxygenases: More than just
636 green chemistry. Chem. Rev. **111**:4165-4222.

- 637 19. **Zhang ZG, Parra LP, Reetz MT.** 2012. Protein engineering of stereoselective Baeyer-
638 Villiger monooxygenases. *Chemistry*. **18**:10160-10172.
- 639 20. **Bornscheuer UT, Huisman GW, Kazlauskas RJ, Lutz S, Moore JC, Robins K.** 2012.
640 Engineering the third wave of biocatalysis. *Nature*. **485**:185-194.
- 641 21. **Ellis HR.** 2010. The FMN-dependent two-component monooxygenase systems. *Arch.*
642 *Biochem. Biophys.* **497**:1-12.
- 643 22. **McGhie EJ, Littlechild J.** 1996. The purification and crystallisation of 2,5-
644 diketocamphane 1,2 monooxygenase and 3,6-ketocamphane 1,6 monooxygenase from
645 *Pseudomonas putida* NCIMB 10007. *Biochem. Soc. Trans.* 29S.
- 646 23. **McGhie EJ, Isupov MN, Schroder E, Littlechild J.** 1998. Crystallization and
647 preliminary X-ray diffraction studies of the oxygenating subunit of 3,6-ketocamphane
648 monooxygenase from *Pseudomonas putida*. *Acta Cryst.* **D54**:1035-1038.
- 649 24. **Isupov MN, Lebedev AA.** 2008. NCS-constrained exhaustive search using oligomeric
650 models. *Acta Cryst.* **D64**:90-98.
- 651 25. **Kadow M, Saß S, Schmidt M, Bornscheuer UT.** 2011. Recombinant expression and
652 purification of the 2,5-diketocamphane 1,2-monooxygenase from the camphor
653 metabolizing *Pseudomonas putida* strain NCIMB 10007. *AMB Express* **1**:13.
- 654 26. **Kadow M, Loschinski K, Saß S, Schmidt M, Bornscheuer UT.** 2012. Completing the
655 series of BVMOs involved in camphor metabolism of *Pseudomonas putida* NCIMB
656 10007 by identification of the two missing genes, their functional expression in *E. coli*,
657 and biochemical characterization. *Appl. Microbiol. Biotechnol.* **96**:419-429.

- 658 27. **Grogan G, Roberts S, Wan P, Willetts A.** 1993. Camphor-grown *Pseudomonas putida*,
659 a multifunctional biocatalyst for undertaking Baeyer-Villiger monooxygenase-dependent
660 biotransformations. *Biotech. Lett.* **15**:913-918.
- 661 28. **Gagnon R, Grogan G, Levitt MS, Roberts SM, Wan PWH, Willetts AJ.** 1994.
662 Biological Baeyer-Villiger oxidation of some monocyclic and bicyclic ketones using
663 monooxygenases from *Acinetobacter calcoaceticus* NCIMB 9871 and *Pseudomonas*
664 *putida* NCIMB 10007. *J. Chem. Soc. Perkin Trans.* 2537-2543.
- 665 29. **Leisch H, Shi R, Grosse S, Morley K, Bergeron H, Cygler M, Iwaki H, Hasegawa Y,**
666 **Lau PCK.** 2012. Cloning, Baeyer-Villiger biooxidations, and structures of the camphor
667 pathway 2-oxo-3-4,5,5-trimethylcyclopentylacetyl-Coenzyme A monooxygenase of
668 *Pseudomonas putida* ATCC 17453. *Appl. Environ. Microbiol.* **78**:2200-2212.
- 669 30. **Beecher J, Richardson P, Willetts A.** 1994. Baeyer-Villiger monooxygenase-dependent
670 biotransformations: Stereospecific heteroatom oxidations by camphor-grown
671 *Pseudomonas putida* to produce chiral sulfoxides. *Biotechnol. Letts* **16**:909-912.
- 672 31. **Beecher J, Grogan G, Roberts S, Willetts A.** 1996. Enantioselective oxidations by the
673 diketocamphane monooxygenase isozymes from *Pseudomonas putida*. *Biotechnol. Letts*
674 **18**:571-576.
- 675 32. **Beecher J, Willetts A.** 1998. Biotransformation of organic sulfides. Predictive active site
676 models for sulfoxidation catalysed by 2,5-diketocamphane 1,2-monooxygenase and 3,6-
677 diketocamphane 1,6-monooxygenase, enantiocomplementary enzymes from
678 *Pseudomonas putida* NCIMB 10007. *Tetrahedron Asymm.* **9**:1899-1916.
- 679 33. **Gagnon R, Grogan G, Roberts SM, Villa R, Willetts AJ.** 1995. Enzymatic Baeyer-
680 Villiger oxidations of some bicyclo[2.2.1]heptan-2-ones using monooxygenases from

- 681 *Pseudomonas putida* NCIMB 10007: enantioselective preparation of a precursor of
682 azadirachtin. J. Chem. Soc. Perkin Trans. 1505-1511.
- 683 34. **Conrad HE, Hedegaard J, Gunsalus IC, Corey EJ, Uda H.** 1965. Lactone
684 intermediates in the microbial oxidation of (+)-camphor. Tetrahedron Lett. **6**:561-565.
- 685 35. **Trudgill, PW, DuBus R, Gunsalus IC.** 1966a. Mixed function oxidation: V. Flavin
686 interaction with a reduced diphosphopyridine nucleotide dehydrogenase, one of the
687 enzymes participating in camphor lactonization. J. Biol. Chem. **241**:1194-1205.
- 688 36. **Trudgill PW, DuBus R, Gunsalus IC.** 1966b. Mixed function oxidation: VI.
689 Purification of a tightly coupled electron transport complex in camphor lactonization. J.
690 Biol. Chem. 241:4288-4290.
- 691 37. **Pedraza RO, Ricci JCD.** 2002. In-well cell lysis technique reveals two new
692 megaplasmids of 103.0 and 212.6 MDa in the multiple plasmid-containing strain V517 of
693 *Escherichia coli*. Lett. Appl. Microbiol. **34**:130–133.
- 694 38. **Barton BM, Harding GP, Zuccarelli AJ.** 1995. A general method for detecting and
695 sizing large plasmids. Anal. Biochem. 226:235-240.
- 696 39. **Romine MF, Stillwell LC, Wong KK, Thurstone SJ, Sisk EC, Sensen C, Gassterland**
697 **T, Fredrickson JK, Saffer JD.** 1999. Complete sequence of a 184-kilobase catabolic
698 plasmid from *Sphingomonas aromaticivorans* F199. J. Bacteriol. **181**:1585-1602.
- 699 40. **Bergeron H, Labbé D, Turmel C, Lau PCK.** (1998) Cloning, sequence and expression
700 of a linear plasmid-based and a chromosomally homolog of chloroacetaldehyde
701 dehydrogenase-encoding genes in *Xanthobacter autotrophicus* GJ10. Gene **207**:9-18.
- 702 41. **Sambrook J, Fritsch EF, Maniatis T.** 1989. Molecular cloning: a laboratory manual, 2nd
703 ed. Cold Spring Harbor Laboratory Press, Cold Spring Harbor, N.Y.

- 704 42. **Smith SP, Barber KR, Dunn SD, Shaw GS.** 1996. Structural influence of cation
705 binding to recombinant human brain S100b: evidence for calcium-induced exposure of a
706 hydrophobic surface. *Biochemistry* **35**:8805-8814.
- 707 43. **Iwaki H, Hasegawa Y, Wang S, Kayser MM, Lau PCK.** 2002. Cloning and
708 characterization of a gene cluster involved in cyclopentanol metabolism in *Comamonas*
709 sp. strain NCIMB 9872 and biotransformations effected by *Escherichia coli*-expressed
710 cyclopentanone 1,2-monooxygenase. *Appl. Environ. Microbiol.* **68**:5671-5684.
- 711 44. **Iwaki H, Wang S, Grosse S, Bergeron H, Nagahashi A, Lertvorachon J, Yang J,**
712 **Konishi Y, Hasegawa Y, Lau PCK.** 2006. Pseudomonad cyclopentadecanone
713 monooxygenase displaying an uncommon spectrum of Baeyer-Villiger oxidations of
714 cyclic ketones. *Appl. Environ. Microbiol.* **72**:2707-2720.
- 715 45. **Edman P, Henschen A.** 1975. Sequence determination, p. 232-279. In S.B. Needleman
716 (ed.), *Protein Sequence Determination*, Springer, Berlin.
- 717 46. **Mahoney WC, Hermodson MA.** 1979. High-yield cleavage of tryptophanyl peptide
718 bonds by o-iodosobenzoic acid. *Biochemistry.* **18**:3810-3814.
- 719 47. **Skopp RN, Lane LC.** 1988. Fingerprinting of proteins cleaved in solution by cyanogen
720 bromide. *Appl. Theor. Electroph.* **1**:61-64.
- 721 48. **Piszkiwicz D, Landon M, Smith EL.** 1970. Anomalous cleavage of aspartyl-proline
722 peptide bonds during amino acid sequence determinations. *Biochem. Biophys. Res.*
723 *Commun.* **40**:1173-1178.
- 724 49. **Russell TR, Tu SC.** 2004. *Aminobacter aminovorans* NADH:flavin oxidoreductase His
725 140: A highly conserved residue critical for NADH binding and utilization. *Biochem.*
726 **43**:12887-12893.

- 727 50. **Imagawa T, Tsurumura T, Sugimoto Y, Aki K, Ishidoh K, Kuramitsu S, Tsuge H.**
728 2011. Structural basis of free reduced flavin generation by flavin reductase from *Thermus*
729 *thermophilus* HB8. *J. Biol.Chem.* **286**:44078-44085.
- 730 51. **Zhang Y, Edwards TE, Begley DW, Abramov A, Thompkins KB, Ferrell M, Guo**
731 **WJ, Phan I, Olsen C, Napuli A, Sankaran B, Stacey R, van Voorhis WC, Stewart**
732 **LJ, Myler PJ.** 2011. Structure of nitrilotriacetate monooxygenase component B from
733 *Mycobacterium thermoresistibile*. *Acta Cryst.* **F67**:1100-1105.
- 734 52. **Tu SC.** 2001. Reduced flavin: Donor and acceptor enzymes and mechanisms of
735 channeling. *Antioxidants and Redox Signaling.* **3**:881-897.
- 736 53. **Jablonski E, DeLuca M.** 1978. Studies of the control of luminescence in *Beneckea*
737 *harveyi*: Properties of the NADH and NADPH:FMN oxidoreductases *Biochemistry,*
738 **17**:672-678.
- 739 54. **Yu CA, Gunsalus IC.** 1969. Monooxygenases: VII. Camphor ketolactonase I and the
740 role of three protein components. *J. Biol. Chem.* **244**:6149-6152.
- 741 55. **Chakrabarty AM.** 1976. Plasmids in *Pseudomonas*. *Ann. Rev. Genet.* **10**:7-30.
- 742 56. **Aramaki H, Sagara Y, Hosoi M, Horiuchi T.** 1993. Evidence for autoregulation of
743 *camR*, which encodes a repressor for the cytochrome P-450cam hydroxylase operon on
744 the *Pseudomonas putida* CAM plasmid. *J. Bacteriol.* **175**:7828-7833.
- 745 57. **Chaiyen P, Fraaije MW, Mattevi A.** 2012. The enigmatic reaction of flavins with
746 oxygen. *Trends Biotech.* **39**:373-380.

747

748

749

750 **List of Tables**

751

752 Table 1. Oxidation of terpenones

753 Table 2. Kinetic resolution of racemic ketones

754 Table 3. Desymmetrization of prochiral ketones

755 Table 4. Regiodivergent oxidations of bicyclic ketones

756

757 **Figure legends**

758

759 FIG 1. Metabolism of camphor isomers to acetyl-CoA and isobutyryl-CoA in *Pseudomonas*
760 *putida* ATCC 17453. Modified from Leisch et al. (29) with cumulative data from references 7, 9,

761 11. Nomenclature of *camE* for the oxygenating components of diketocamphane (DKC)
762 monooxygenase isozymes (DKCMO) was adapted from Koga et al. (10). Fred is a short-chain

763 flavin reductase (this study). The lactones of DKC monooxygenations are presumed to undergo
764 spontaneous hydrolysis to form compound **5** (9). *camF1/F2* are putative genes for 2-oxo- Δ^3 -

765 4,5,5-trimethylcyclopentenylacetyl-CoA synthetase (Fig. S1 in supplemental material) that
766 produce the carbonyl-CoA (COSCoA) derivative of **5**, a substrate for OTEMO (type 1 BVMO;

767 29). HSCoA, acetyl-CoA. Additional steps of the degradation pathway are in discussed in Fig.
768 S1 of supplemental material.

769

770 FIG 2. Localization of additional genes and predicted open reading frames (ORFs) flanking the
771 established initial genes of the camphor *camDCAB* operon and its repressor, *camR* on a ~40.5-kb
772 sequenced region of the CAM plasmid of *P. putida* ATCC 17453. The predicted ORFs or genes

773 are numbered from 1-27 except for the established *camRDCAB* that are shaded in black. The
774 orientation of the arrows indicates the direction of gene transcription. The candidate genes of
775 this study (*camE*_{25-1; 25-2} and *camD*₃₆) representing the three diketocamphane monooxygenase
776 (DKCMO) isozymes are highlighted in grey. The previously established OTEMO-encoding gene
777 (29) has been designated *camG* following the respective catabolic steps (see Fig. 1). *camS*, *T*, *U*
778 and *V* are potential transcriptional regulators, *camV* is a close homolog of *camR*. Rationale for
779 the predicted ORFs and the various subclones and the probe regions to cover the sequenced
780 CAM plasmid locus are elaborated in the SM1/Table S1/S2/Fig. S1 of supplemental material. The
781 black solid line represents the previously sequenced region with the indicated GenBank
782 accession numbers.

783
784 FIG 3. Establishing linearity of CAM plasmid of *P. putida* ATCC17453 by pulsed field gel
785 electrophoresis. Lane 1. Lambda ladder PFG marker DNA with some indicated size in kb
786 alongside; Lanes 3 and 5 are S1-nuclease treated *S. aromaticivorans* and CAM plasmid DNA
787 preparations, respectively. Lanes 2 and 4 are S1 nuclease–non treated samples of *S.*
788 *aromaticivorans* F199 and CAM plasmid DNAs, respectively. A, B and C indicate the estimated
789 plasmid sizes of CAM plasmid (533-kb) of strain PpCam, pNL2 (485-kb) and pNL1 (185-kb) of
790 strain F199, respectively.

791
792 FIG 4. Purification scheme and SDS-PAGE (12% PA) of 18-kDa FMN-reductase (Fred) from *P.*
793 *putida* ATCC 17453. Units of enzyme activity are defined by the amount of protein which
794 oxidizes one μ mole of NADH ($\epsilon = 6.22 \text{ L mmol}^{-1} \text{ cm}^{-1}$) per min using FMN as substrate. Protein

795 standards (ovalbumin, carbonic anhydrase, lysozyme) of decreasing sizes are indicated
796 alongside. The purified Fred as shown is after the final size exclusion step.

797

798

799 FIG 5. Protein sequence alignment of PpCam flavin reductase (Fred) with short-chain flavin
800 reductases of known structures with top scores from the PDB entries. 3NFW, nitrilotriacetate
801 monooxygenase component B of *Mycobacterium thermoresistibile*, 40.5% identity; 3PFT, flavin
802 reductase (DszD) of *M. goodii*, 29.8% identity; 1RZ0, flavin reductase (PheA2) of phenol 2-
803 hydroxylase of *Bacillus thermoglucosidasius* A7, 28.8% identity; and 2ECR, flavin reductase
804 (HpaC) of hydroxyphenylacetate 3-monooxygenase of *Thermus thermophilus* HP8, 25.1%
805 identity. The secondary structural elements of 3NFW are indicated and labelled above the
806 aligned sequences. The predicted secondary structural elements of Fred using the Psipred
807 program (<http://bioinf.cs.ucl.ac.uk/psipred/>) are shown below. The consensus amino acids of the
808 aligned sequences including ten entirely conserved residues are highlighted.

809

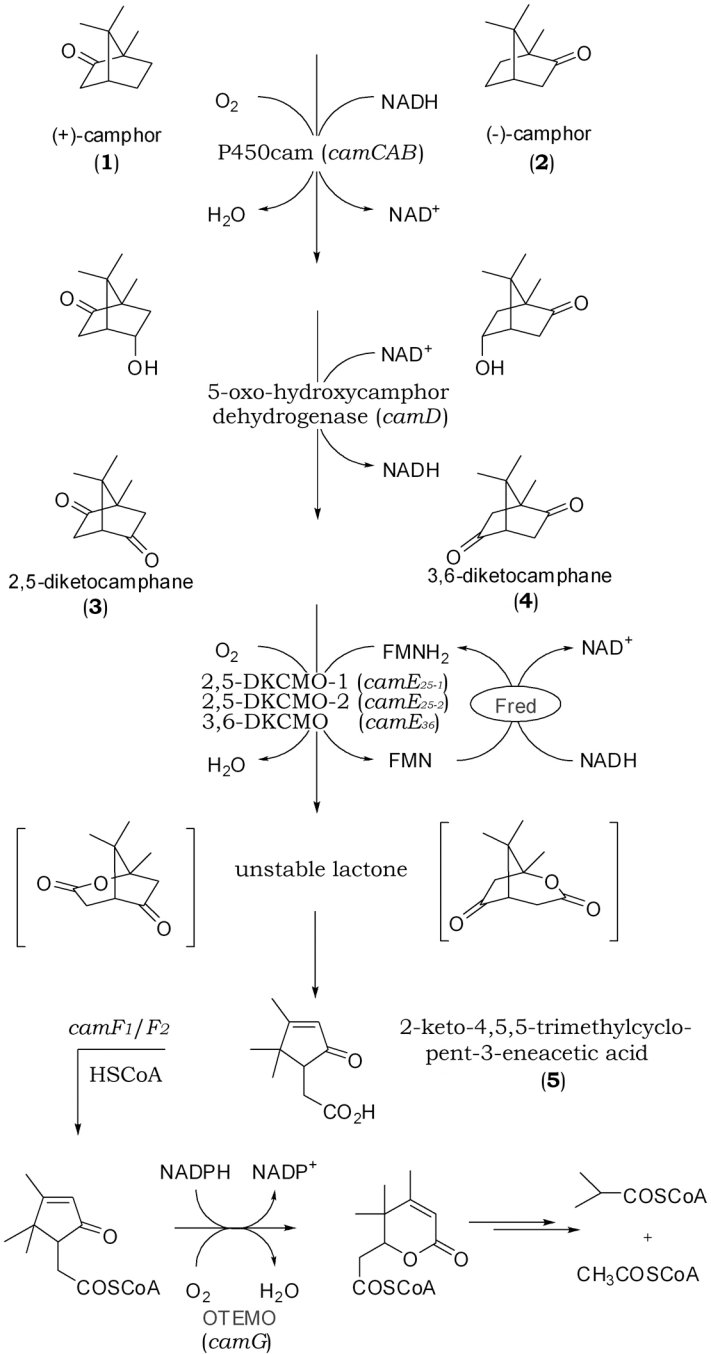
810 FIG 6. Potentiation of 2,5-DKCMO activity by the addition of FMN-reductase (Fred).

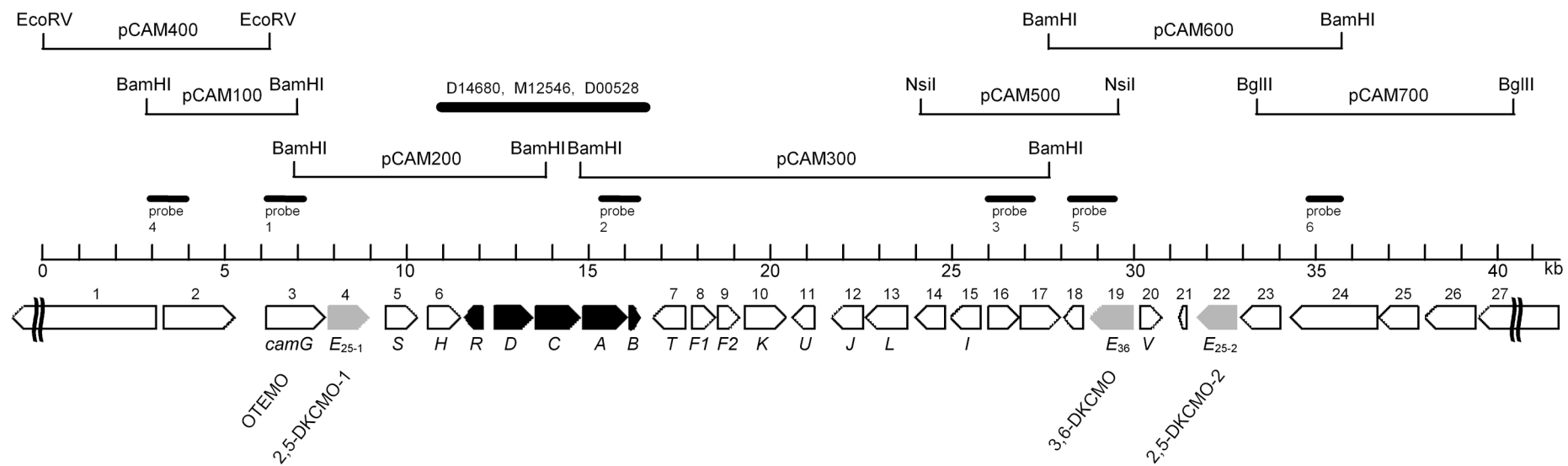
811 Remaining (+)-camphor (●) was monitored by HPLC with a constant amount of 2,5-DKCMO-2
812 while increasing the Fred concentration. Reaction incubation time was 30 min. The resulting
813 increment in DKCMO activity is as indicated (▼).

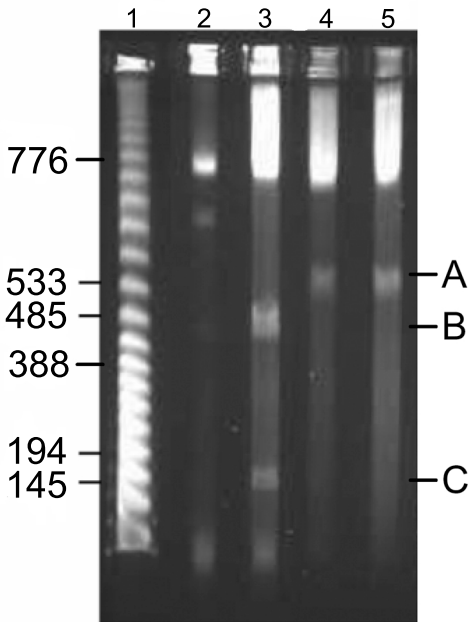
814

815

816





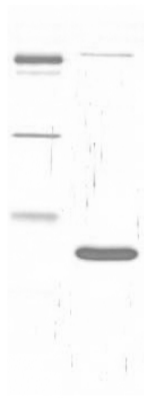


M_r (kDa)

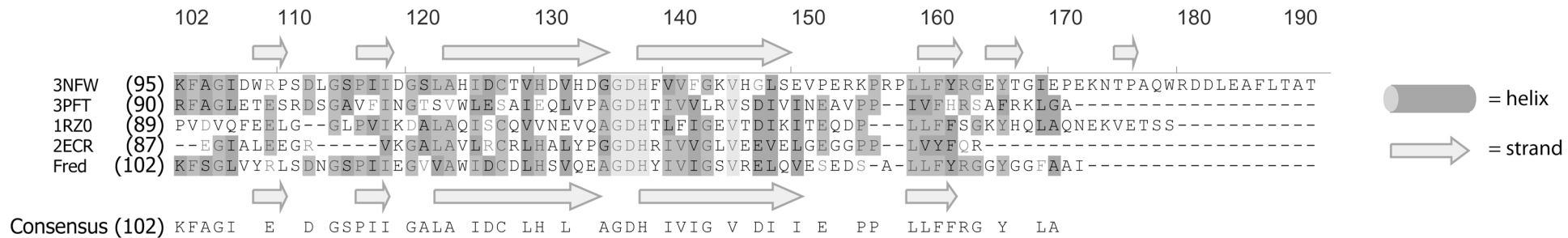
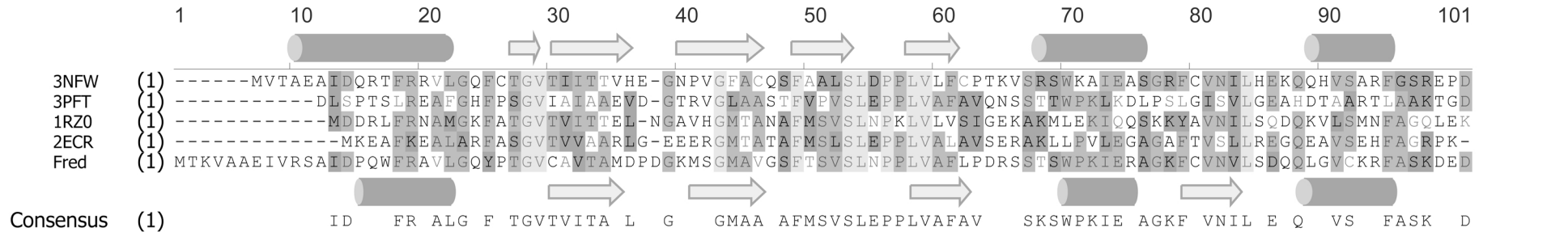
45 -

31 -

21 -



Purification step	Tot. Prot. (mg)	Tot. Act. (U)	Spec. Act. (U/mg)	Yield/Purif. (% / fold)
Crude extract	4,200	10,080	2.4	100 / 1
DEAE-Seph.	160	4,692	29.2	47 / 12
Ni-NTA	18	3,248	176.9	32 / 74
Superdex 200	3	1,791	628.4	18 / 262



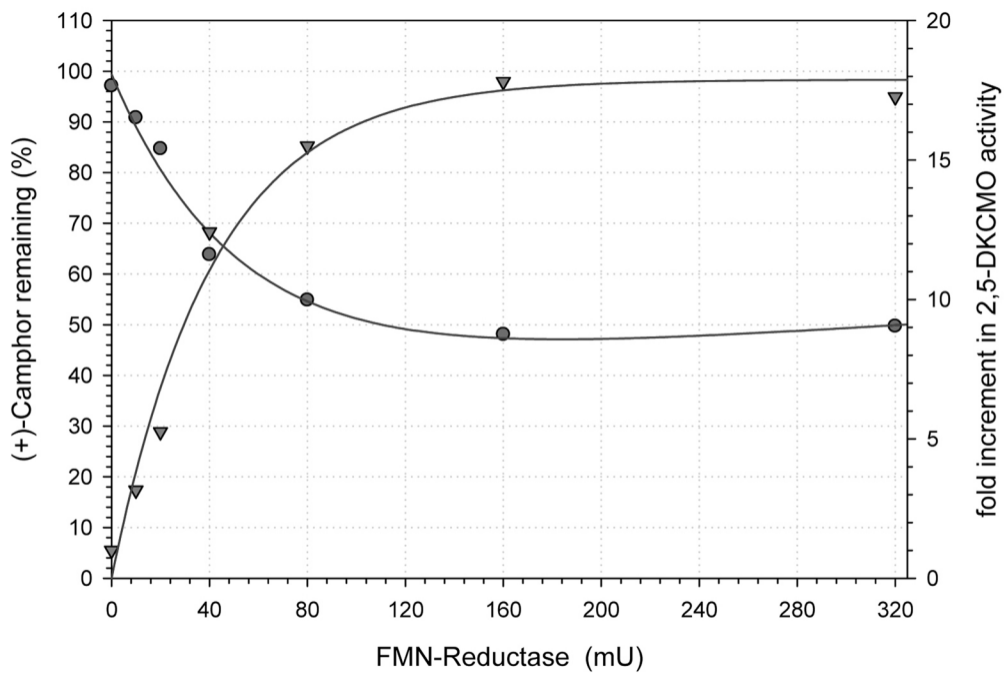


Table 1. Oxidation of terpenones

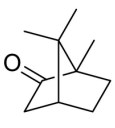
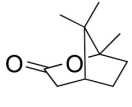
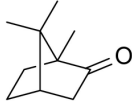
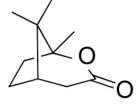
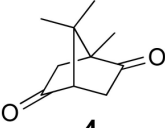
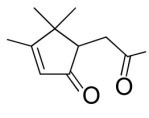
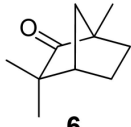
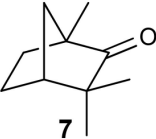
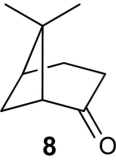
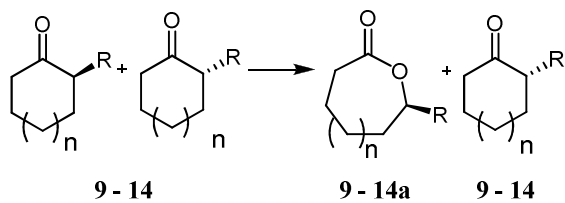
Substrate	2,5-DKCMO-1 +Fred	2,5-DKCMO-2 +Fred	3,6-DKCMO + Fred	Product
 1	100%	100%	0%	 1a
 2	0%	0%	100%	 2a
 4	0%	0%	100%	 5
 6		No conversion		
 7		No conversion		
 8		No conversion		

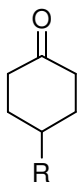
Table 2. Kinetic resolution of racemic ketones



Substrate			2,5-DKCMO-1 +Fred		2,5-DKCMO-2 +Fred		3,6-DKCMO +Fred	
#	n	R	Conv. ^a %	<i>E</i> ^b	Conv. %	<i>E</i>	Conv. %	<i>E</i>
9	1	Me	8	3.2 (<i>S</i>)	4	3.1 (<i>S</i>)	2	3.2 (<i>S</i>)
10	1	Et	11	43 (<i>S</i>)	6	22 (<i>S</i>)	0	n.a. ^c
11	1	Pr	18	19 (<i>S</i>)	13	8.5 (<i>S</i>)	trace	n.a.
12	1	Ph	23	>200 (<i>R</i>)	4	>200 (<i>R</i>)	2	1
13	0	Me	0	n.a.	0	n.a.	0	n.a.
14	0	He	6	12 (<i>S</i>)	3	5 (<i>S</i>)	0	n.a.

^a determined by chiral GC based on area percentage; ^b Values were calculated according to a program available at <http://biocatalysis.uni-graz.at/pub/enantio/>; ^c not available.

Table 3. Desymmetrization of prochiral ketones.

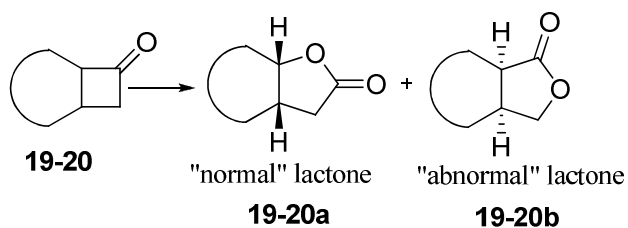


- 15** R = methyl
16 R = ethyl
17 R = *n*-pentyl
18 R = *tert*-butyl

Subst.	2,5-DKCMO-1 + Fred		2,5-DKCMO-2 + Fred		3,6-DKCMO + Fred	
	Conv. ^a %	<i>ee</i> ^b %	Conv. %	<i>ee</i> %	Conv. %	<i>ee</i> %
15	8	27 (<i>R</i>)	5	55 (<i>R</i>)	Traces	n.a. ^c
16	29	71 (<i>R</i>)	10	89 (<i>R</i>)	3	87 (<i>S</i>)
17	2	26 (<i>R</i>)	traces	n.a.	0	n. a.
18	5	61 (<i>S</i>)	traces	n.a.	0	n.a.

^a determined by chiral GC based on area percentage; ^b determined by chiral GC; ^c not available.

Table 4. Regiodivergent oxidations of bicyclic ketones.



Substrate	Biocat.	Conv. %	"normal" lactone	"abnormal" lactone
 19	2,5-DKCMO-1 + Fred	100	ratio 1.3 : 1	
			77% ee (1 <i>R</i> ,5 <i>S</i>)	99% ee (1 <i>S</i> ,5 <i>R</i>)
	2,5-DKCMO-2 + Fred	100	ratio 1.1 : 1	
			87% ee (1 <i>R</i> ,5 <i>S</i>)	97% ee (1 <i>S</i> ,5 <i>R</i>)
	3,6-DKCMO + Fred	53	ratio 1 : 1.5	
			57% ee (1 <i>R</i> ,5 <i>S</i>)	93% ee (1 <i>S</i> ,5 <i>R</i>)
 20	2,5-DKCMO-1 + Fred	64 ^a	ratio 2.4 : 1	
			40% ee (1 <i>R</i> ,5 <i>S</i>)	57% ee (1 <i>R</i> ,5 <i>S</i>)
	2,5-DKCMO-2 + Fred	59 ^b	ratio 1.8 : 1	
			58% ee (1 <i>R</i> ,5 <i>S</i>)	20% ee (1 <i>R</i> ,5 <i>S</i>)
	3,6-DKCMO + Fred	26 ^c	only normal lactone	
			94% ee (1 <i>R</i> ,5 <i>S</i>)	0

^a. Starting material 98% ee; ^b. Starting material 89% ee; ^c. Starting material 45% ee